Geophys. J. Int. (1995) **121,** 532–544

Neural network analyses of stress-induced overpressures in the Pannonian Basin

R. Van Balen and S. Cloetingh

Tectonics/Structural Geology Group, Institute of Earth Sciences, Vrije Universiteit, de Boelelaan 1085, 1081 *HV Amsterdam, The Netherlands*

Accepted 1994 November 9. Received 1994 November 8; in original form 1994 March 8

SUMMARY

Artificial neural networks can learn relationships between sediment characteristics (burial depth, composition, coordinates and thickness of overlying Quaternary deposits) and overpressures from well data, after which they can interpolate and extrapolate to areas and depths not covered by wells. We analyse data from the south-eastern part of the Pannonian Basin. We use a neural network for analysing fluid overpressures because of the complex interaction of the key variables, making it difficult to derive the functional relationships required for a statistical analysis. The optimal topology of the network (number of hidden layers and neurons) is found by minimizing the network's training and testing errors. The optimal design of the network resembles the interactions scheme of the key variables.

The Pannonian Basin, originally formed in an extensional regime, has been in a compressive state of stress since Late Pliocene, causing anomalous subsidence patterns. Numerical forward modelling of compaction-driven fluid overpressures shows that, due to an increase in the level of compressive interplate stress, the fluid overpressures in the deep subbasins have increased substantially since Late Pliocene, giving rise to a very high overpressure (up to 45 MPa) at present. The neural network analyses provide an independent estimate of the current amount of overpressuring in this basin, complementing the numerical forward modelling results. The overpressure profiles obtained by the two modelling approaches are in excellent agreement, showing the same magnitude of overpressures, a reversal of the overpressure in the deepest parts of the subbasins and a general decrease of the overpressure from SW to NE.

Key words: basin analyses, compaction, intraplate stress, neural network, overpressure, Pannonian Basin.

INTRODUCTION

The Pannonian Basin is a Middle Miocene extensional basin located inside the Alpine chain. The deepest parts of the basin, the Mako Trough and Békés Basin, are completely filled by deltaic sediments, consisting of marls, siltstones, sandstones and conglomerates. In general, hydrostatic fluid pressures are present down to a depth of about 1800 m, below which significant overpressures occur (Szalay 1982, 1988; Clayton *et al.* 1990). The overpressures originate from sedimentary loading, causing pore size reductions (compaction), and low permeability of sediments, which restricts the escape of the pore fluid. During Late Pliocene–Quaternary times, the subsidence in the central part of the Pannonian Basin (Great Hungarian Plain) accelerated, whereas the peripheral parts were uplifted, inducing a relative sea-level rise in the centre and a relative fall at the flanks of the basin. This pattern of differential subsidence and uplift can be explained by the bending of the lithosphere due to an increase in the level of compressive lithospheric stress since Late Pliocene (Horváth & Cloetingh 1995; Van Balen & Cloetingh 1994; Van Balen *et al.* 1995). The acceleration of subsidence causes sedimentation rates to increase. As shown by the results of numerical forward modelling by Van Balen & Cloetingh (1994) and Van Balen *et al.* (1995), this stress-induced increase of sedimentation rates has caused a dramatic increase in the amount of overpressure in the two deepest subbasins since Late Pliocene, resulting in a very high overpressure (up to 45 MPa) at present (Szalay 1982). As the hydrocarbon generation started between 9 and 6 Ma

ago (Horváth *et al.* 1987; Szalay 1988), this basin-wide hydrodynamic change will have affected the hydrocarbon migration. In addition, a basin-wide cementation event will have occurred, because diagenesis of sediments is very sensitive to changes in the fluid regime of sedimentary basins (Horbury & Robinson 1993).

We use a neural network method for mapping, interpolation and extrapolation of fluid overpressures in the south-eastern part of the Pannonian Basin. The trained networks are used to predict the overpressure along a cross-section, which is compared to the results of numerical forward modelling of the same profile (Van Balen & Cloetingh 1994; Van Balen *et al.* 1995).

NEURAL NETWORKS

Artificial neural networks are software tools inspired by brain models, which are used for pattern recognition purposes (Sejnowski, Koch & Churchland 1988). They are capable of learning, i.e. they can find relationships in data. Artificial neural networks learn by 'investigating' a set of training data. Once the relationship in these data has been found, not only can they reproduce the learned data but also interpolate and extrapolate to new values. They are now widely used for recognition (sound, image, etc.) and interpolation and extrapolation (mapping, weather prediction, etc.) purposes. Neural networks have been used by earth scientists for reserve estimates (Wu & Zhou 1993), mapping (Hagens & Doveton 1991; Penn, Gordon & Wentlandt 1993; Ritter & Hepner 1990), predicting lithologies from well logs (Rogers *et al.* 1992) and forecasting geomagnetic activity (Hernandez, Tajima & Worton 1993). Although neural networks are parallel by nature, as a program they can run on sequential computers like PCs and workstations (Eberhart & Dobbins 1990).

For data analysis purposes, artificial neural networks provide an alternative to statistical regression methods because they can find functional relationships in data sets without any *a priori* knowledge about their form (linear, exponential, etc.). Even kriging, the most sophisticated statistical interpolation method, needs, apart from the plain data, information about the data distribution (Davis 1986; Olea 1992). A semivariogram has to be provided by the data analyst, which is produced by a 'trial and error process, usually done by eye' (Davis 1986), possibly giving rise to biassing caused by the subjective mind of the researcher. Robinson (1991) compares the performances of a neural network to a standard statistical regression method on an artificial data set. The network is better at making predictions than the regression method, due to the fact that the latter needs information on the type of function sought. Noise in the data set makes it difficult to 'guess' this function and, if the dependent variable is a function of two or more parameters, estimating the form of this function is hampered by graphical representation problems. According to Hecht-Nielsen (1990), enough experimental evidence has now been gathered to state that the back-propagation neural network is, in general, comparable to the best non-linear statistical regression methods.

An artificial neural network consists of highly interconnected simple processing units called neurons. Information

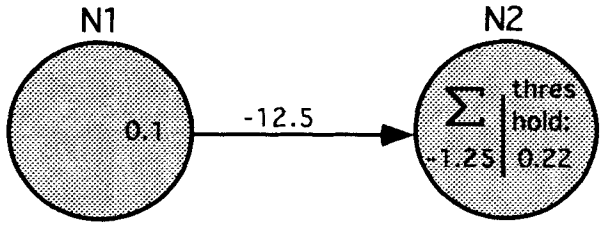

Figure 1. Transport of information between neurons is accomplished by multiplying the value of the input neurons by the value of the connection weight between the neurons.

in the network is stored by the value of the weights of the connections between neurons and the layout of the connection network (Hecht-Nielsen 1990; Freeman & Skapura 1991). The value of the weight of a connection represents its 'goodness' (negative values are inhibitive, positive values excitative). Each neuron has four components: input connections (synapses), a summation function, a threshold function and output connections (Eberhart & Dobbins 1990; Hecht-Nielsen 1990; Freeman & Skapura 1991). The transport of information between neurons is accomplished by multiplying the value of the inputting neuron by the weight of the connection between the neurons (see Fig. 1). The value of a neuron is determined by applying a threshold function to the summation of all input information and is a value in the range of 0 and 1 (see Fig. 2). Data are fed into the network by assigning values to input neurons. These are subsequently passed through the network. The values of the output neurons give the response of the network to the pattern presented to the input neurons.

Back-propagation neural networks

The most widely used form of neural network for mapping problems (finding a function in data) is based on the principle of back-propagation of errors. In this type of network, the neurons are organized in layers: one input layer, one output layer and one or more so-called hidden layers (Fig. 3). The network is fully interconnected, i.e. every neuron is connected to all neurons in the one (for input and output layer neurons) or two (for hidden layer neurons) neighbouring layers, but neurons in the same layer cannot communicate with each other (Fig. 3). Information flows in one direction: from the input neurons towards the output neurons (feedforward). Although the values of the hidden units and connection weights are not of crucial importance for the user of the network, they are often

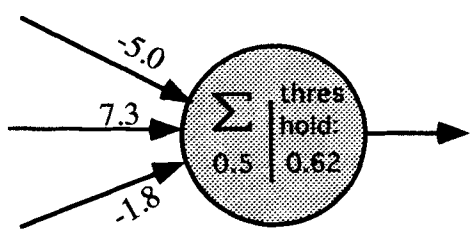

Figure 2. The summation function applied on total input to neuron.

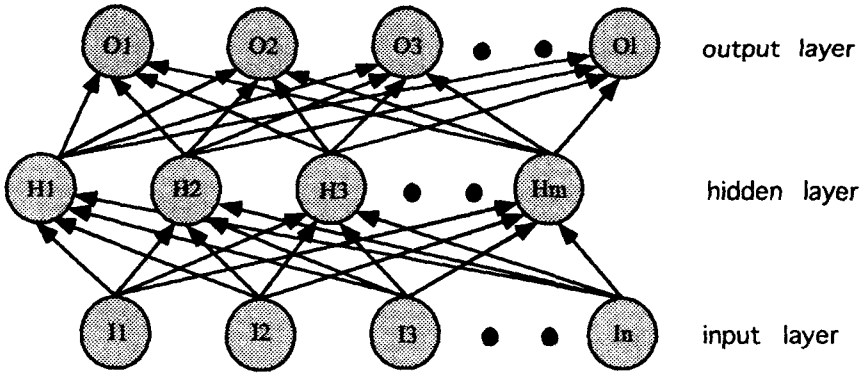

Figure 3. A typical back-propagation neural network layout. The flow of information is from the input to the output neurons (feedforward).

inspected to see how the network achieves generalizations (Rumelhart, Hinton & Williams 1986; Touretzki & Pomerleau 1989). In back-propagation networks, learning is accomplished by comparing the output of the network with the desired (known) output. The difference between the two is a measure for the changes in the values of the connection weights needed in order to improve the network's performance (Rumelhart *et al.* 1986; Jones & Hoskins 1987; Hecht-Nielsen 1990; Freeman & Skapura 1991).

The number of neurons in the input and output layers is fully determined by the research problem. A neural network may contain several hidden layers, although usually one or two hidden layers are enough (Sejnowski *et al.* 1988; Freeman & Skapura 1991; Robinson 1991). It is proved mathematically that, given enough neurons in the hidden layer, a back-propagation network with only one hidden layer is capable of approximating any function from one finite dimensional space to another (Hornik, Stinchcombe & White 1989). However, it has not been proven that any known learning algorithm can actually find the associated perfect values for the connection weights (Hecht-Nielsen 1990). The optimum number of hidden layers and neurons has to be found by an iterative procedure. In general, the larger the number of hidden layers and neurons, the easier it will be for the network to 'learn' the data, but at the same time less generalization is achieved causing a poor performance of the network on a test data set (Rumelhart *et al.* 1986; Hecht-Nielsen 1990; Robinson 1991). Networks with too few neurons in the hidden layers will not be able to find patterns in the data. The optimum number of hidden layers and neurons arises when the network is 'just' capable of learning the data, ensuring the network has made a proper generalization (Hecht-Nielsen 1990; Robinson 1991).

Network training

Building a neural network model involves two steps. In the first step, the learning phase, the network is shown the training input and output patterns. The network learns by comparing predicted and known output patterns. In the second step, the testing phase, the network only sees the testing input patterns. The predicted and known output patterns are compared and a testing error is computed. Because the network tends to forget the patterns it has just learned (i.e. every new pattern changes the weights in a different way than its precursors) an iteration is required for training the network successfully. The iteration consists of repeating the two steps until the minimum testing error has been found. If this error is still too large, the network did not generalize properly on the training data and the whole process is repeated with a different network topology.

The most common training error minimization technique used is the gradient descent method and derivatives of it. In order to break the symmetry, the weights in the network are initialized with random values.

Pursuing an error minimum during the learning phase can lead to overtraining the network: the network is trained to fit the observed data perfectly, but is very bad at generalization. Overtraining starts when the error curve begins to level out (the convergence rate of the network decreases); at this point the training should be terminated (Hecht-Nielsen 1990). Typically, continuation of training results in a decrease of the mean squared error of the training data, whereas it increases for the test data set.

THE PANNONIAN BASIN

Origin and fill of the Pannonian Basin

The Pannonian Basin is a large Neogene intramontane sedimentary basin located inside the Alpine chain. It is surrounded by the eastern Alps, the Carpathians and the Dinarides (see Fig. 4a). The basin covers parts of Austria, Hungary, Rumania, Slovakia, Slovenia, Serbia and the Czech Republic. The basin's basement consists of Palaeozoic and Mesozoic metamorphic rocks, stacked on top of each other during the Cretaceous alpine collision (Csontos *et al.* 1992). Locally a Palaeogene retro-arc basin underlies the Neogene series (Tari, Horváth & Rumpler 1992). The basin originates from large-scale Middle Miocene (Badenian) strike-slip tectonics, which are related to tectonic escape from the eastern Alps (Ratschbacher *et al.* 1991), mantle diapirism (Stegena, Géczy & Horváth 1975; Becker 1993) and subduction roll-back along the Carpathian front (Stegena *et al.* 1975). The extension in the basin is manifested by the formation of pull-apart basins, flower structures (positive and negative), rifts and metamorphic core complexes (Bergerat 1989; Horváth *et al.* 1988; Royden 1988; Tari *et al.* 1992). The basin has an extremely high heat flow (up to 120 mW m^{-2}) (Dövényi & Horváth 1988), a very thin lithosphere (60 km) (Stegena *et al.* 1975; Sclater *et al.*

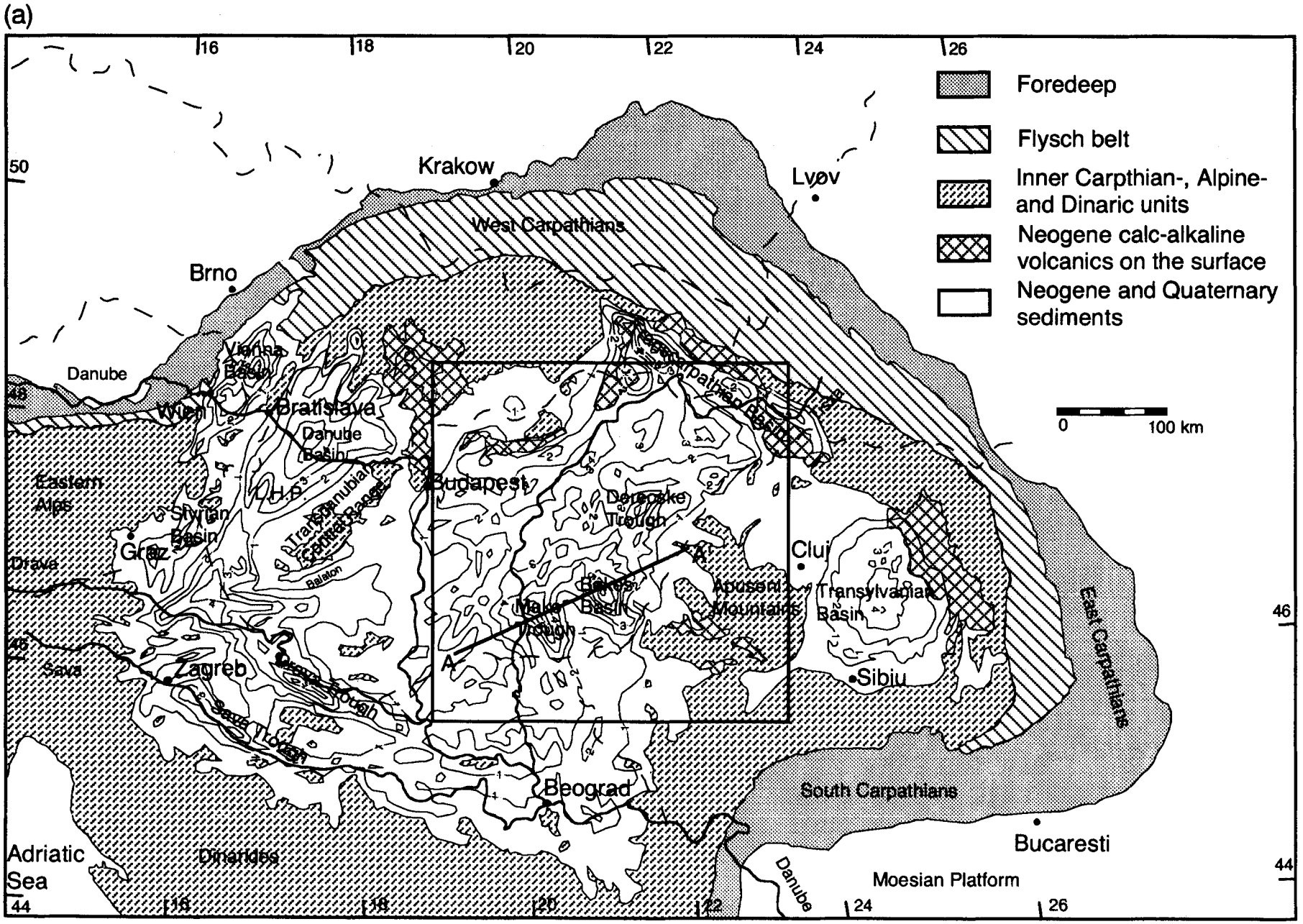

Figure 4. (a) The Pannonian Basin and its surroundings (after Horváth 1993). The inset shows the position of Fig. 4(b). A–A′ denotes the modelled cross-section. (b) The locations of the wells used in these analyses.

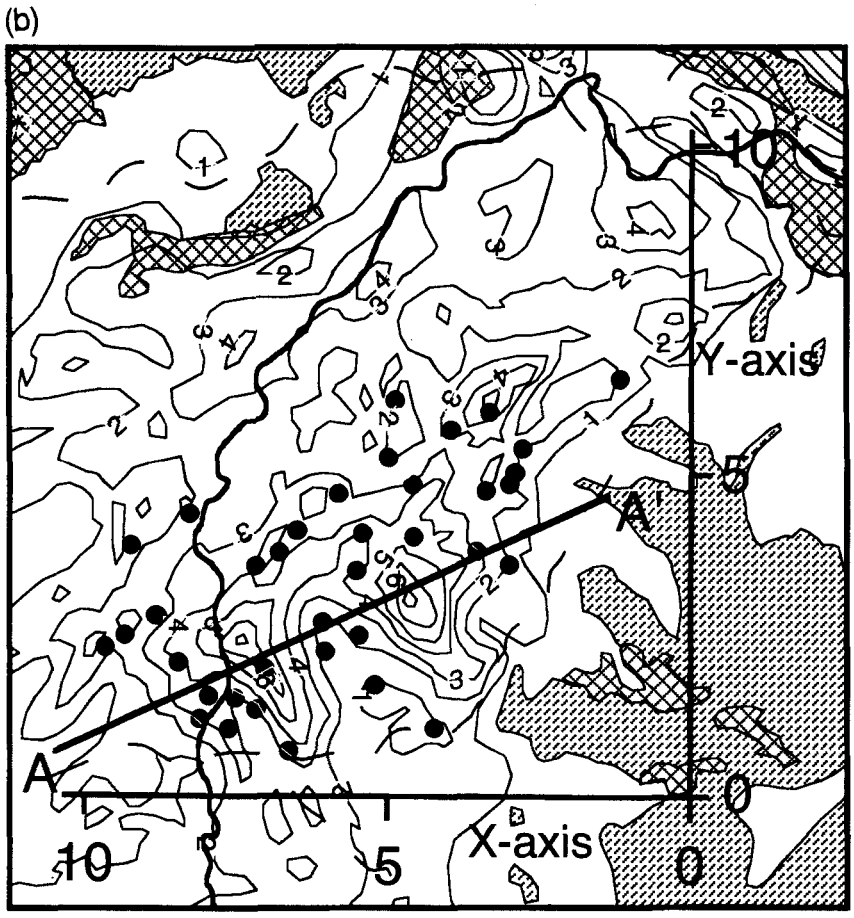

Figure 4. (*Continued.*)

1980) and a small positive Bouguer gravity anomaly (Bielik 1988).

During the whole post-rift period the Pannonian Basin was a lake, with water depths reaching more than 1 km at the end of the rifting period (Horváth *et al.* 1988; Kázmér 1990), giving rise to sediment starvation (Grow *et al.* 1989) and euxenic conditions (Kázmér 1990). A large delta system moving from the Carpathians towards the deep subbasins (Great Hungarian Plain) completely filled the basin by the end of the Pliocene (Kázmér 1990).

Hydrocarbon generation and migration in the Pannonian Basin

The main source rocks for hydrocarbons in the Pannonian Basin are Miocene and Early Pliocene marls. Mesozoic and Palaeogene deposits contribute small amounts of source rocks (Dank 1988; Šarković, Stanković & Miloslavljević 1991). The Miocene marl deposits are generally overpressured in the Pannonian Basin (Clayton *et al.* 1990). Overpressures measured at the rims of the Békés Basin are up to 15 MPa, while in the Mako Trough the maximum measured overpressure is around 45 MPa. Modelling of maturation and overpressuring (Horváth *et al.* 1987; Szalay 1988) shows that the hydrocarbon generation started between 9 and 6 Myr ago. Significant overpressures started to develop more or less at the same time. The high overpressure and a possible change of the overall stress field (Horváth *et al.* 1987) resulted in local tensile hydrofracturing of the basement. These fractures are sometimes filled with hydrocarbons. The most common hydrocarbon traps are compactional anticlines over basement highs (Dank 1988). In the south-eastern part of the Pannonian basin the three major hydrocarbon occurrences are located at the margins of the deep subbasins (Makó Trough and Békés Basin) in compactional anticlines.

Stress-induced overpressures in the Pannonian Basin

Observations of the present-day lithospheric stress field in and around the Pannonian Basin (Fig. 5) show that it is in a compressive state of stress (Müller *et al.* 1992; Becker 1993). As demonstrated by Cloetingh, McQueen & Lambeck (1985), such a compressive stress bends the lithosphere, causing differential uplift and subsidence across sedimentary basins, giving rise to relative sea-level changes at the same time-scale and magnitude as second- and third-order eustatic sea-level changes (Cloetingh 1991). This model is used by Horváth and Cloetingh (1994) and Van Balen *et al.* (1995) to explain the observed anomalous Late Pliocene–Quaternary subsidence in the Pannonian Basin in terms of an increase in the level of compressive stress since Late Pliocene.

The effect of this increase in the level of compressive intraplate stress on the compaction-driven fluid flow regime in the two deepest subbasins in the Pannonian Basin (Mako

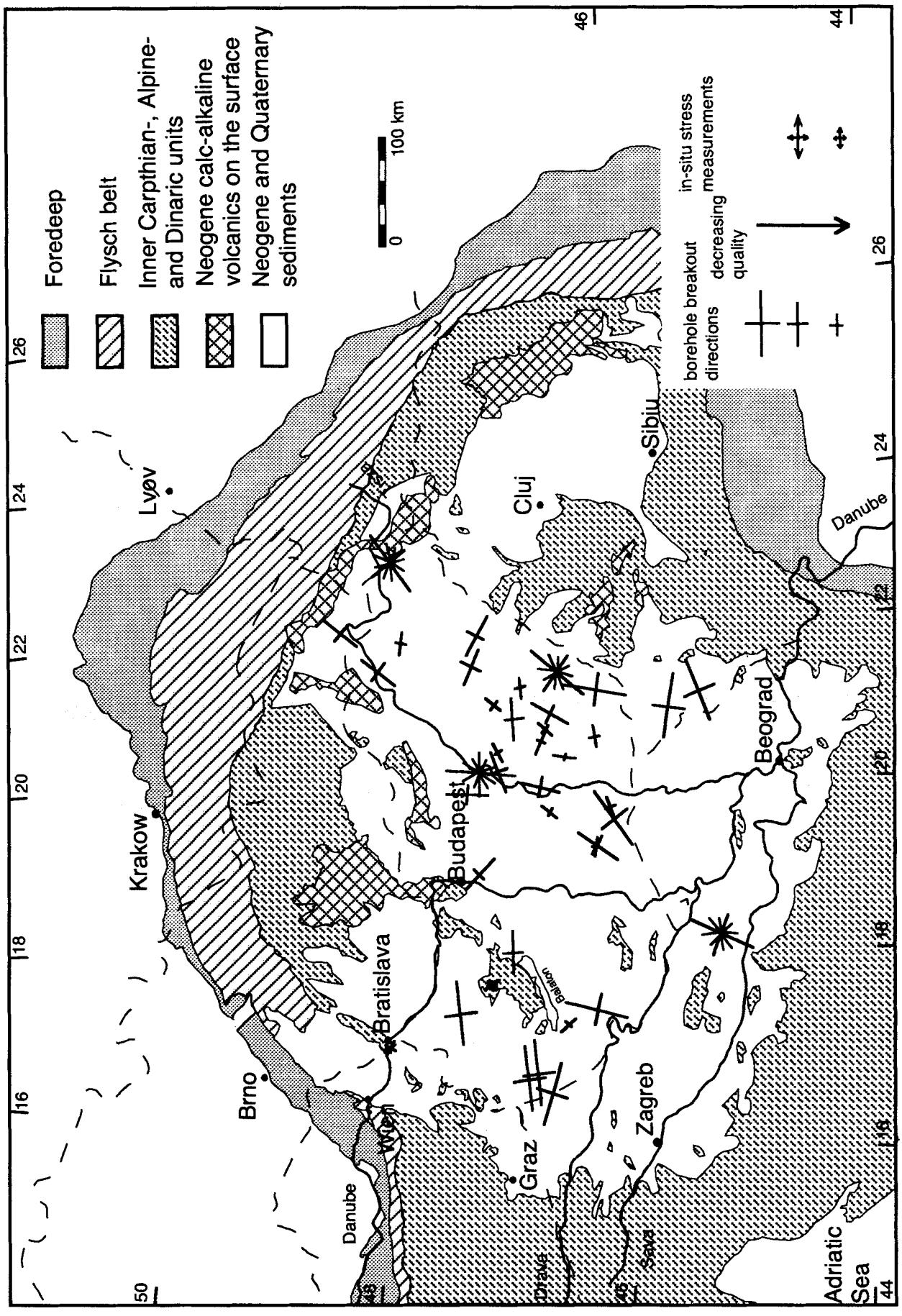

Figure 5. The stress map for the Pannonian Basin (Becker 1993; Müller *et al.* 1992) showing the consistent SW–NE directions of the maximum horizontal stress.

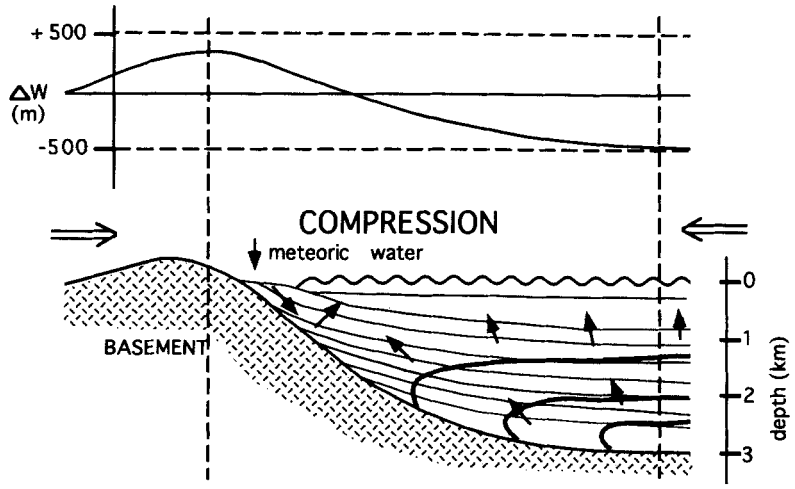

Figure 6. The effect of an increase in the level of compressive intraplate stress on the hydrodynamics of a sedimentary basin. The upper panel shows the lithospheric deflection (ΔW) resulting from the compression. The stress-induced flank uplift causes an increased gravity potential and exposure of sediments at the margin, enhancing meteoric water infiltration. Compression-enhanced basin centre subsidence results in higher sedimentation rates and therefore promotes the development of compaction-driven fluid overpressuring (after Van Balen & Cloetingh 1994).

Trough and Békés Basin) is discussed by Van Balen and Cloetingh (1994) and Van Balen *et al.* (1995). Their forward numerical model is based on the lithospheric stretching models of McKenzie (1978) and Kooi, Cloetingh & Burrus (1992) and links lithospheric strength and extension, thermal subsidence, flexural isostasy, horizontal lithospheric forces and sedimentary fill processes to the compaction-driven hydrodynamics of sedimentary basins (Van Balen & Cloetingh 1993). They demonstrate that the current high amount of overpressure in the two deepest subbasins can be explained by the same increase in the level of compressive in-plane stress that caused the anomalous Pliocene–Quaternary subsidence (Fig. 6). The maximum amount of overpressure in the Mako Trough prior to the compressive stress event is 21 MPa. It increases during a time interval of 1.5 Myr to a value of 36 MPa at the peak stress conditions, and presently, after a total time span of 3.9 Myr, reaches a maximum of 45 MPA. In addition, their results show a systematic decrease of the overpressure from the Mako Trough towards the Békés Basin.

ARTIFICIAL NEURAL NETWORK ANALYSES OF OVERPRESSURES IN THE PANNONIAN BASIN

Input parameters

The number of input and output neurons for the artificial neural network is determined by the characteristics of the research problem. In our case there is one output neuron, representing the overpressure. The number of input neurons is given by the number of parameters influencing the fluid overpressure in sedimentary basins in general and the Pannonian Basin in particular. We have defined five of these parameters, resulting in five input neurons. The relationships between these parameters and the fluid overpressure is indicated in Fig. 7. The input parameters are discussed below. In a separate test, all five parameters were found to be significantly influencing the results. Compaction-induced fluid overpressuring is caused by external loading of porous

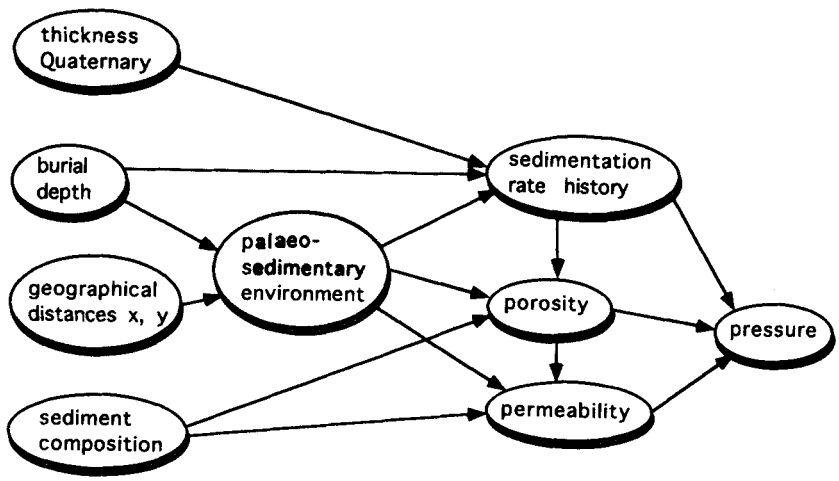

Figure 7. Scheme depicting the relationships between the input parameters and the fluid overpressure (see text for a discussion).

sediment, in this case by the weight of the overburden. Loading causes the pores to decrease their volume, in response to which the pore fluid builds up an overpressure. This pressure is relaxed by flow of the pore fluid from high to low overpressure zones. The rate of this flow is determined by amongst others the porosity and permeability of the sediments involved, and controls the relaxation rate of the overpressure. Therefore, key parameters for fluid overpressuring in sedimentary basins are the overburden load, porosity and permeability.

Burial depth gives an upper limit to the amount of overpressuring (the lithostatic pressure or overburden weight) and is related to the compaction history by comprising the sedimentation (loading) rate history and the palaeosedimentary environment (for example, a deep part of the basin is very likely to contain deep basin sediments, i.e. clays or marls). In the Pannonian Basin the overpressure shows a very distinctive positive correlation with burial depth (see Fig. 8a), starting from a depth of about 2 km. Notice that the trend could be linear, piecewise linear or exponential.

Hydraulic characteristics of sediments (i.e. permeability and porosity) are largely determined by the sediment composition (sandstone, shale, carbonate, etc.). For example, a sandstone is (in general) highly permeable and has a high porosity compared to a shale. Also, sediment composition encompasses the palaeosedimentary environment (for example, sandstones can be deposited in alluvial plains, beaches and basin floor fans, but generally not at delta slopes). The sediments of the south-eastern part of the Pannonian Basin can be generalized to a mixture of marls and sandstones (Mattick, Philips & Rumpler 1988). We did not have access to sediment composition data. Instead, we have related the composition to lithostratigraphic units by assigning a fixed sand percentage to them: 1.0 for the basal sandstone, 0.0 for the deep basin marls, 0.2 for the turbidites and slope sediments and 0.8 for the alluvial plain deposits (see Mattick *et al.* 1988). This gives rise to noise in the learning data set. The effect of this noise on the performance of the neural network will be discussed later. Sediment composition, expressed as the percentage of sand in the sediments, shows a negative correlation with the overpressure (see Fig. 8b).

Sedimentation rates vary strongly across a delta system:

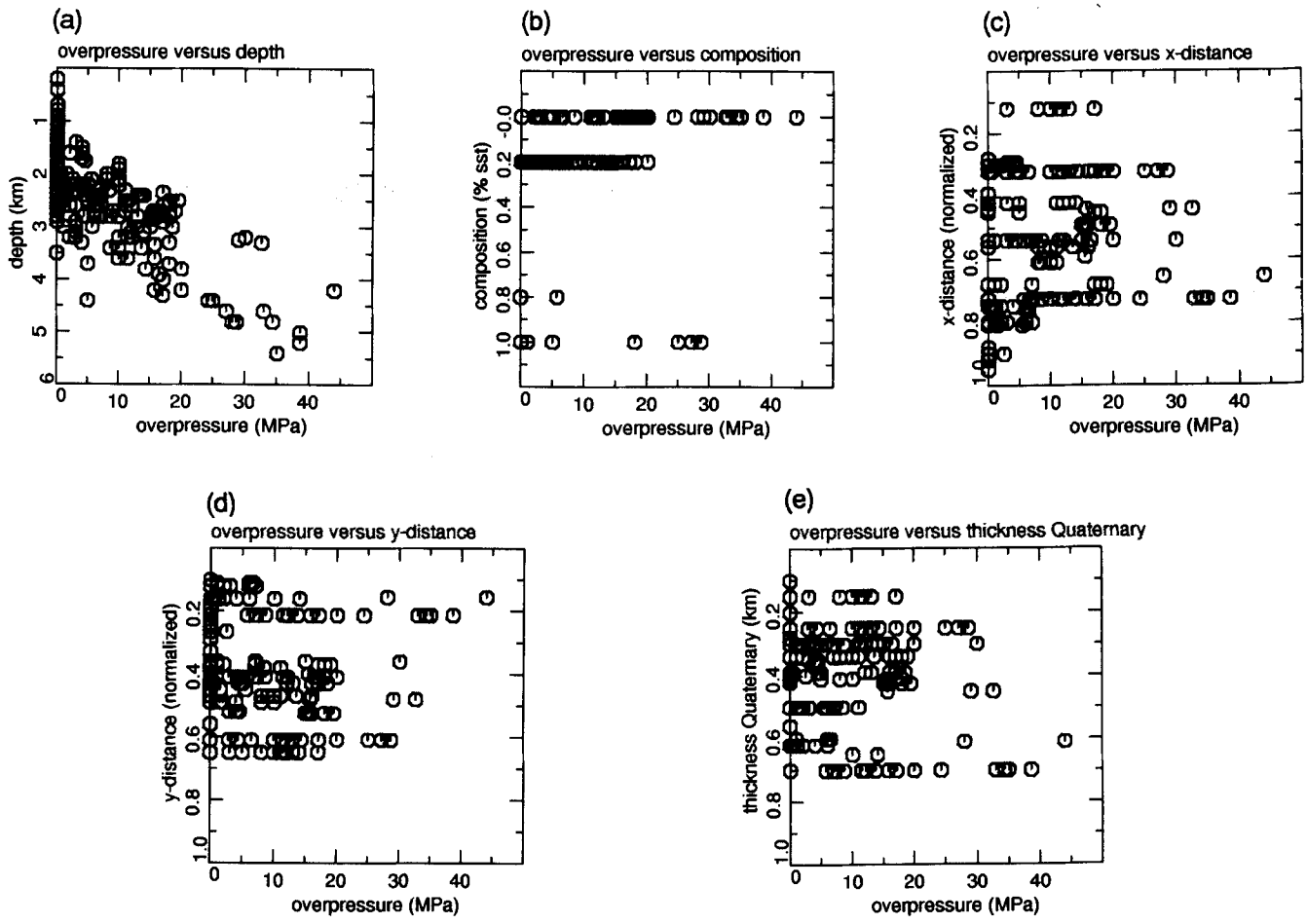

Figure 8. Correlation graphs showing the relationships between the input parameters and the overpressure in the assembled data base. (a) Overpressure versus depth, showing a linear, piecewise linear or exponential trend; (b) overpressure versus composition (expressed in percentage of sandstone); (c,d) overpressure versus distance, the distance being measured using the coordinate axes depicted in Fig. 4(b); (e) overpressure versus thickness of the overlying Quaternary deposits.

the delta slope has the highest deposition rate, which decreases in landward and basinward directions. The Pannonian delta system moved from the Carpathians towards the deep subbasins (Kázmér 1990). Therefore, the sedimentation rates were not the same in the whole basin during its total history, but varied in space and time. As a result, the overpressure is a function of distance. As can be seen in Figs 8(c) and (d), for the coordinate axes we have defined, a positive correlation exists between the x-coordinate and the overpressure and a negative correlation occurs between the y-coordinate and the amount of overpressure.

Finally, because of the anomalous basin subsidence during Late Pliocene and Quaternary, we use the thickness of the Quaternary deposits as the fifth input parameter. The thickness of these sediments relates directly to the youngest sedimentation (loading) rates. A positive correlation between the thickness of these sediments and the amount of overpressure is quite evident in Fig. 8(e). The age of the sediments would be a good sixth parameter, but unfortunately, the absolute ages are largely unconstrained.

Neurons can operate on values within a limited range, in this case between 0 and 1. Therefore, the five input parameters and the output value have to be transformed to this range. As there is no unique transformation, this should be done very carefully, ensuring the whole 0 to 1 range of the neurons is used and that a proper resolution is obtained. For the burial depth, 10 km is the maximum value. Therefore, depth is mapped to the 0 or 1 domain by dividing it by a value of 10. Sediment composition is given by the percentage of sandstone in the deposit, which correlates in a natural way to the neuron's value range. The x- and y-coordinates, having a maximum of 10 distance units, are also divided by 10 in order to map them to the 0 to 1 domain. The thickness of the Quaternary deposits does not exceed 1 km; therefore, these values do not have to be transformed. Finally, the observed overpressures have a minimum of 0.0 MPa and a maximum of about 45 MPa. As a consequence, they are divided by 50.

Data sources

The learning and testing data set for the network analysis is compiled from different sources. Fluid overpressure data for several wells are reported in Szalay (1982, 1988) and Clayton *et al.* (1990). Additional overpressure data come from Horváth and Lenkey (1993, private communication). The wells used in this study are indicated in Fig. 4(b). In this part of the Pannonian Basin there is only one well which reaches a depth of 5.4 km: Hod-I located in the centre of the Mako Trough. All the other wells are much shallower; typical depths are 2–3 km. As can be seen in Fig. 4(b), the deep part of the Békés Basin is not penetrated by a well. For this subbasin we only have information about the overpressure for the outer, shallower part. As will be shown below, neural network analysis enables extrapolation down to a depth of 6 km in this subbasin.

Sediment compositions (the percentage of sandstone in the deposits) for the lithostratigraphic units in the south-eastern part of the Pannonian Basin are based on Mattick *et al.* (1988). The distribution, thickness and depth of these lithostratigraphic units are given by Juhász (1991). The thickness and distribution of the Quaternary deposits are presented by Rónai (1974). Finally, the coordinate axes we have defined are indicated in Fig. 4(b).

Using these sources, we have assembled a data base with 193 records containing the output and five input parameters. During training of the network 150 patterns (data records) were used, while the remaining 43 patterns were used to compare the predicted and known overpressures during the testing phase. The input data which are required when the trained neural network is used to predict overpressures (interpolation and extrapolation) along a profile through the Pannonian Basin (burial depths, sediment composition, coordinates and thickness of overlying Quaternary sediments) are assembled from the same sources as the training and testing input data.

Results

We have tested networks with one, two and three hidden layers, containing varying numbers of hidden neurons. The networks were trained to the minimum squared error for the test data set. For every step of 0.001 mean squared training error, the connection weights were saved and the testing mean squared error was computed. Theoretically, the mean squared error for the test data set decreases during training until the moment that overtraining of the network takes place. From this point, upon decreasing the training error, the testing error increases (Hecht-Nielsen 1990). We consider the values of the weights of the network at this point as optimal. A plot of the training error versus testing error for five different networks is shown in Fig. 9. This figure illustrates that the second smallest network with one

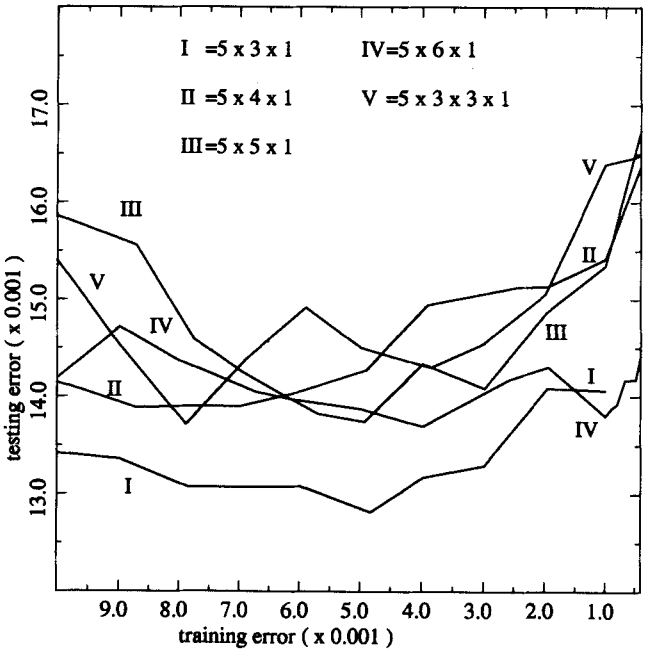

Figure 9. Training versus testing errors for five different network topologies. In general, a decrease of the training error induces first the testing error to decrease also, until the point where the network becomes overtrained (i.e. it tends to memorize the training data). From this point the testing error increases. The graphs for the smallest and larger sized networks could not be plotted due to the large testing errors.

hidden layer and three hidden neurons (the $5 \times 3 \times 1$ network) has the best performance because it obtains the lowest testing error. The results for the $5 \times 2 \times 1$, $5 \times 4 \times 3 \times 1$, $5 \times 3 \times 2 \times 1$ and $5 \times 4 \times 2 \times 1$ networks could not be plotted in this figure due to their high testing errors (>0.018). Predicted versus known overpressures for the best networks are shown in Fig. 10.

The performances of the networks can be understood by considering their degrees of freedom. The smallest network, $5 \times 2 \times 1$, does not have enough degrees of freedom and is, therefore, forced to too much generalization, leading to a bad performance on both the training and testing data. In contrast, the larger sized networks have too many degrees of freedom and are, therefore, bad at generalization and require larger training data sets.

From inspection of the scheme depicting the relationships between the input parameters and the overpressure (Fig. 7), it becomes clear why the $5 \times 3 \times 1$ network yields an optimal performance. In this scheme, there are four intermediate variables which relate the input parameters to the overpressure, and one of them (the palaeosedimentary environment) might be collapsed into the other three (i.e. it is not an independent variable), resulting in three intermediate variables. Presumably these three variables coincide with the three hidden neurons in the $5 \times 3 \times 1$ network.

Figure 11 displays the results obtained when the $5 \times 3 \times 1$ network is used to predict the overpressure profile. A comparison of the results of forward numerical modelling, shown in Fig. 12, with the profile generated by the $5 \times 3 \times 1$ network, demonstrates that they are in excellent agreement. The amount and location of overpressure maxima, taking into account the uncertainties in both types of modelling, agree very well. Both neural network analyses and forward numerical modelling show that the overpressure decreases at the deepest part of the subbasins, in the basal sandstone unit. Also, both methods predict a trend of decreasing overpressures going from the Mako Trough to the Békés Basin. This can be explained by the thicknesses of the youngest deposits, which indicate a higher sedimentation rate above the Mako Trough during Quaternary times. This phenomenon is related to the distribution of vertical lithospheric loads, which determine the response of the lithosphere to the increase in the level of compressive intraplate stress. They cause the maximum of stress-induced subsidence to be located exactly above the Mako Trough (Van Balen & Cloetingh 1994; Van Balen *et al.* 1995).

Owing to lack of data, sediment composition has to be

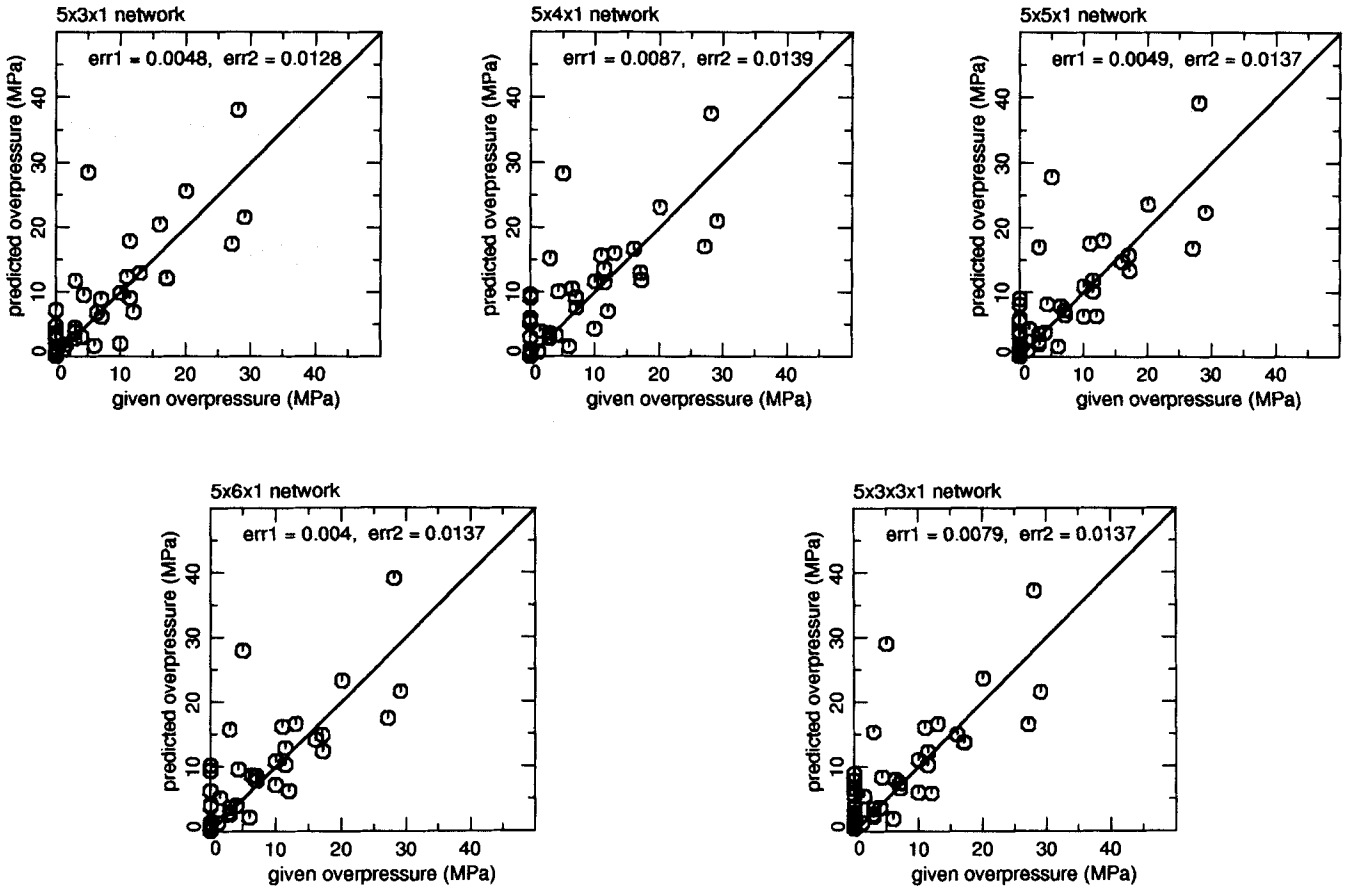

Figure 10. Observed versus predicted overpressures for the best networks. Err1 is the mean squared training error, err2 the mean squared testing error. The data estimates that have predicted values in excess of the observations relate to marls whose pore fluids have possibly leaked along high permeable conduits like faults. The overpressure data with predicted values less than actually observed are basal sandstones. These could represent sandstone bodies that are sealed by marls.

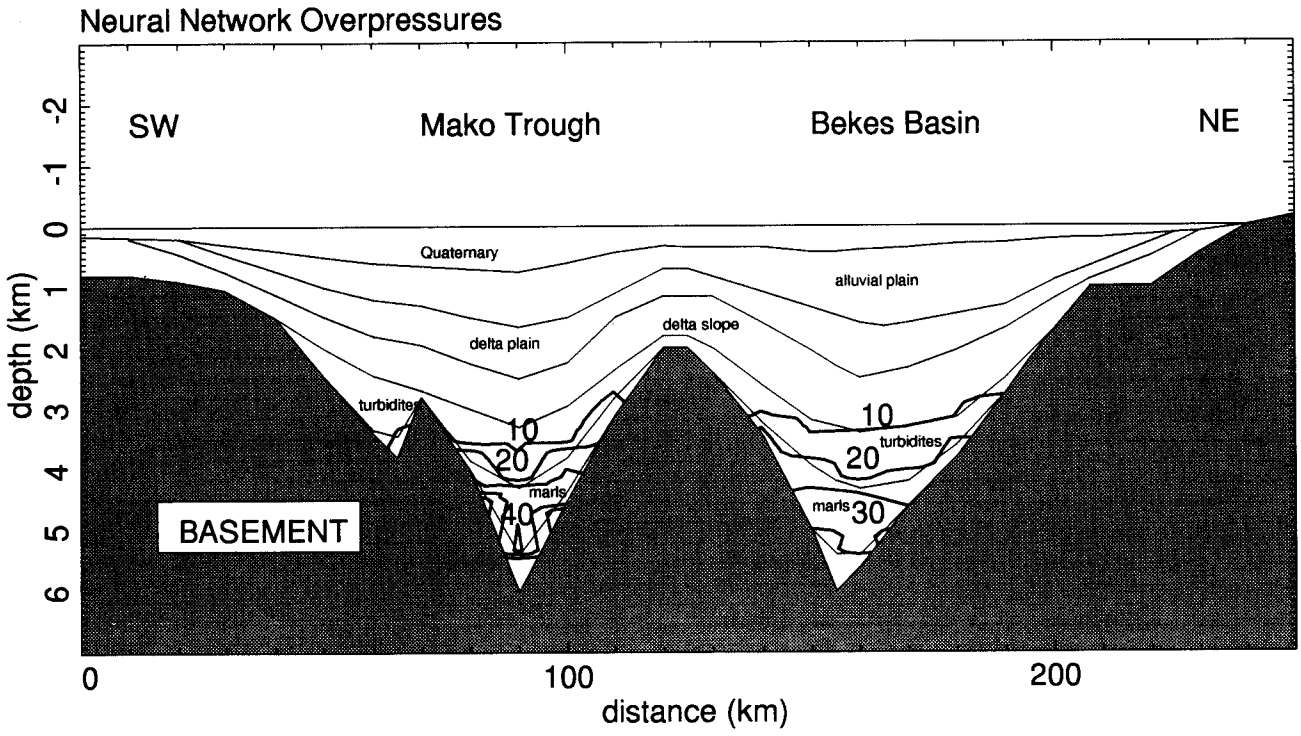

Figure 11. Overpressure through the Mako Trough and Békés Basin produced by the $5 \times 3 \times 1$ neural network. Thick lines are contour lines for the overpressures (MPa), thin lines represent the stratigraphy. An overpressure reversal occurs in the deepest part of the subbasins. Generally, the overpressures in the Mako Trough are less than in the Békés Basin.

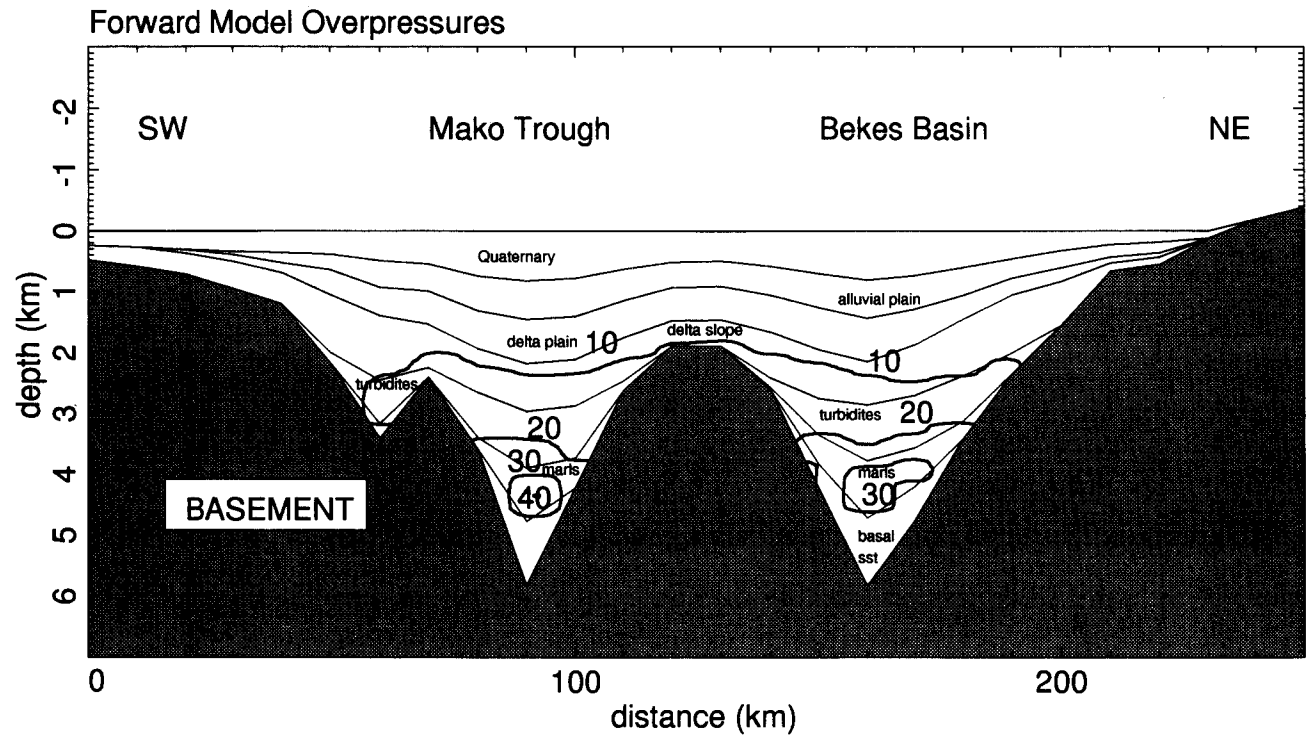

Figure 12. Overpressure profile predicted by numerical forward modelling (after Van Balen *et al.* 1995), showing similarities to the overpressure profiles obtained by the neural network analyses. Thick lines are contour lines for the overpressure (MPa), thin lines represent the modelled stratigraphy. The modelled overpressure profile also shows the overpressure reversal and slightly less overpressure in the Békés Basin inferred from the neural network analyses.

estimated. This gives rise to noise in the data. A second source of data scattering is the uncertainty in the fluid overpressure data. Most of them are derived from mud weights in drilling wells. Furthermore, in our analyses for the basin-wide characteristics we assume that the overpressure constitutes a continuous field. On a subbasin scale, due to localized thermal expansion, hydrocarbon generation and leakage and sealing along faults, this is obviously a simplification. Taking all the noise in the data into account, it is very surprising that the neural networks are able to find the correct patterns in the data. It was noted earlier that artificial neural networks are insensitive to noise in data. Our findings demonstrate that they can extract the big picture through all the noise (Freeman & Skapura 1991).

CONCLUSIONS AND DISCUSSION

Neural networks are universal approximaters; they can perform any mapping between variables. Compared to statistical regression techniques, their great advantage is that they can find the mapping function themselves, no matter how complex it is. Neural networks have been applied successfully to many geophysical problems. We have used neural networks to predict overpressures along a cross-section in the Pannonian Basin. The overpressure data in this basin are scattered and most of them are shallow (2–3 km). Deep data are available in only one well. However, our results show that, despite noise in the training data, neural networks are capable of interpolating and extrapolating the overpressures, i.e. the resulting overpressure profile is in agreement with results obtained by numerical forward modelling.

A relatively small sized network, having one hidden layer with three neurons, is found to be optimal for extrapolating and interpolating the data. This can be explained by examining the relationships between the input parameters and the overpressure: three or four intermediate variables can be defined. Larger networks probably have too many degrees of freedom, requiring larger training sets. The smaller network does not have enough degrees of freedom and is, therefore, forced to too much generalization.

As shown in both numerical forward modelling and neural network analyses, the overpressure decreases at the deepest parts of the subbasins, in the basal sandstone unit. The amount of overpressure is, however, not equal in the subbasins. Both methods predict an overpressure in the Békés Basin which is slightly less than the overpressure in the Mako Trough. This can be explained by spatial variations in the thickness of the Quaternary deposits. As the Quaternary is thicker in the Mako Trough, sedimentation rates during the Quaternary above this subbasin were higher in the Békés Basin, inducing faster compaction. The thickness of the Quaternary deposits can be explained by compression-induced lithospheric deflection since Late Pliocene. Owing to the distribution of vertical lithospheric loads, the maximum of stress-induced subsidence is located exactly above the Mako Trough.

ACKNOWLEDGMENTS

We thank Patrick Ko Shu-pui for the use of his PC neural network program and Drew Van Camp, Tony Plate and Geoffrey Hinton for the neural network simulator for Sun workstations. Fred Beekman is thanked for his help with the software installation. Ferenc Horváth & Laszlo Lenkey have provided overpressure data. Marlies ter Voorde is thanked for constructive discussions and for reviewing an earlier version of this paper. This research was funded by the IBS (Integrated Basin Studies) project, part of the JOULE II research programme funded by the Commission of European Communities (contract no. JOU2-CT 92-0110). IBS contribution No. 19, Publication No. 941106 of the Netherlands Research School of Sedimentary Geology.

REFERENCES

Becker, A., 1993. Contemporary state of stress and neotectonic deformation in the Carpathian–Pannonian region, *Terra Nova*, **5**, 375–388.

Bergerat, F., 1989. From pull-apart to the rifting process: the formation of the Pannonian Basin, *Tectonophysics*, **157**, 271–280.

Bielik, M., 1988. Analyses of the stripped gravity map of the Pannonian Basin, *Geol. Carp.*, **39**, 99–108.

Clayton, J.L., Spencer, C.W., Koncs, I. & Szalay, A., 1990. Origin and migration of hydrocarbon gases and carbon dioxides, Békés Basin, southeastern Hungary, *Organic Geochem.*, **15**, 233–247.

Cloetingh, S., 1991. Tectonics and sea level changes a controversy?, in *Controversies in Modern Geology: A Survey of Recent Developments in Sedimentation and Tectonics*, pp. 249–277, eds Müller, D., Weissel, H. & McKenzie, J.A., Academic Press, London.

Cloetingh, S., McQueen, H. & Lambeck, K., 1985. On a tectonic mechanism for regional sea level variations, *Earth planet. Sci. Lett.*, **75**, 31–61.

Csontos, L., Nagymarosy, A., Horváth, F. & Kovác, M., 1992. Tertiary evolution of the Intra-Carpathian area: a model, *Tectonophysics*, **208**, 221–241.

Dank, V., 1988. Petroleum geology of the Pannonian Basin, Hungary: an overview, *Am. Assoc. Petrol. Geol. Mem.*, **45**, 319–331.

Davis, J.C., 1986. *Statistics and Data Analysis in Geology*, 2nd edn, John Wiley, New York.

Dövényi, P. & Horváth, F., 1988. A review of temperature, thermal conductivity, and heat flow data for the Pannonian Basin, *Am. Assoc. Petrol. Geol. Mem.*, **45**, 195–233.

Eberhart, R.C. & Dobbins, R.W., 1990. *Neural Network PC Tools*, Academic Press, New York.

Freeman, J.A. & Skapura, D.M., 1991. *Neural Networks, Algorithms, Applications, and Programming Techniques*, Addison-Wesley, New York.

Grow, J.A., Pogácsás, G.Y., Bérczíné, M.A., Várnai, P., Hajdu, D., Varga, E. & Péró, C., 1989. A Békési medence tektonikai és szerkezeti viszonyai (Tectonics and structural conditions of the Békés basin), *Magy. Geofiz.*, **30**, 63–97 (with English abstract).

Hagens, A. & Doveton, J.H., 1991. Application of a simple cerebellar model to geologic surface mapping, *Comp. Geosci.*, **17**, 561–567.

Hecht-Nielsen, R., 1990. *Neurocomputing*, Addison-Wesley, New York.

Hernandez, J.V., Tajima, T. & Worton, W., 1993. Neural net forecasting for geomagnetic activity, *Geophy. Res. Lett.*, **20**, 2707–2710.

Horbury, A.D. & Robinson, A.G., (eds) 1993. Diagenesis and basin development, *Am. Assoc. Petrol. Geol. Studies in Geology*, **36**, Tulsa, USA.

Hornik, K., Stinchcombe, M. & White, H., 1989. Multilayer

feedforward networks are universal approximeters, *Neural Networks*, **2**, 359–366.

Horváth, F., 1993. Towards a kinematic model for the Pannonian Basin, *Tectonophysics*, **226**, 333–357.

Horváth, F. & Cloetingh, S., 1995. Anomalous subsidence and uplift in the late stage evolution of the Pannonian Basin, *Geology*, submitted.

Horváth, F., Dövenyi, P., Papp, S., Szalay, A. & Hargitay, M., 1987. Tectonic control on migration and trapping of hydrocarbons in the Pannonian Basin, in *Migration of Hydrocarbons in Sedimentary Basins*, pp. 667–681, ed. Doligez, B., Editions Technip, Paris.

Horváth, F., Dövenyi, P., Szalay, A. & Royden, L., 1988. Subsidence, thermal, and maturation history of the Great Hungarian Plain, *Am. Assoc. Petrol. Geol. Mem.*, **45**, 355–372.

Jones, W.P. & Hoskins, J., 1987. Back-propagation—a generalized delta learning rule, *Byte*, **12**, 155–162.

Juhász, G., 1991. Lithostratigraphical and sedimentological framework of the Pannonian (s.l.) sedimentary sequence in the Hungarian Plain (Alföld), Eastern Hungary, *Acta Geol. Hung.*, **34**(1/2), 53–72.

Kázmér, M., 1990. Birth, life and death of the Pannonian Lake, *Palaeogeog., Palaeoclimat. Palaeoecol.*, **79**, 171–188.

Kooi, H., Cloetingh, S. & Burrus, J., 1992. Lithospheric necking and regional isostasy at extensional basins 1. Subsidence and gravity modelling with an application to the Gulf of Lions margin (SE France), *J. geophys. Res.*, **97**, 17 553–17 571.

Mattick, R.E., Philips, R.L. & Rumpler, J., 1988. Seismic stratigraphy and depositional framework of sedimentary rocks in the Pannonian Basin, southeastern Hungary. *Am. Assoc. Petrol. Geol. Mem.*, **45**, 117–146.

McKenzie, D.P., 1978. Some remarks on the development of sedimentary basins, *Earth Planet. Sci. Lett.*, **40**, 25–32.

Müller, B., Zoback, M.L., Fuchs, K., Mastin, L., Gregersen, S., Pavoni, N., Stephanson, O. & Ljunggren, C., 1992. Regional patterns of tectonic stress in Europe. *J. geophys. Res.*, **97**, 11 783–11 803.

Olea, R.A., 1992. Kriging, understanding allays intimidation, *Geobyte*, **7**, 12–17.

Penn, B.S., Gordon, A.J. & Wendtlandt, R.F., 1993. Using neural networks to locate edges and linear features in satellite images, *Comp. Geosci.*, **19**, 1545–1565.

Ratschbacher, L., Frisch, W., Linzer, H. & Merle, O., 1991. Lateral extrusion in the Eastern Alps, part 2: structural analyses, *Tectonics*, **10**, 257–271.

Ritter, N.D. & Hepner, G.F., 1990. Application of an artificial neural network to land-cover classification of thematic mapper imagery, *Comp. Geosci.*, **16**, 873–880.

Robinson, R., 1991. Neural networks offer an alternative to traditional regression, *Geobyte*, **7**, 14–19.

Rogers, S.J., Fang, J.H., Karr, C.L. & Stanley, D.A., 1992. Determination of lithology from well logs using a neural network, *Am. Assoc. Petrol. Geol. Bull.*, **76**, 731–739.

Rónai, A., 1974. Size of Quaternary movements in Hungary's area, *Acta Geol. Acad. Scient. Hung.*, **18**, 39–44.

Royden, L.H., 1988. Late Cenozoic tectonics of the Pannonian Basin system, *Am. Assoc. Pet. Geol. Mem.*, **45**, 27–48.

Rumelhart, D.E., Hinton, G.E. & Williams, R.J., 1986. Learning representations by back-propagating errors, *Nature*, **323**, 533–536.

Šarković, M., Stanković, S. & Miloslavljević, S., 1991. Petroleum geology of the southeastern part of the Pannonian Basin, *Terra Nova*, **3**, 550–554.

Sclater, J.G., Royden, L., Horváth, F., Burchfiel, B.C., Semken, S. & Stegena, L., 1980. The formation of the Intra-Carpathian basins as determined from subsidence data, *Earth planet. Sci. Lett.*, **51**, 139–162.

Sejnowski, T.J., Koch, C. & Churchland, P.S., 1988. Computational neuroscience, *Science*, **241**, 1299–1306.

Stegena, L., Géczy, B. & Horváth, F., 1975. Late Cenozoic evolution of the Pannonian Basin, *Tectonophysics*, **26**, 71–90.

Szalay, A., 1982. A rekonstrukciós szemléletü földtani kutatás lehetöségei a szénhidrogén-perspektivák elörejelzésében (Possibilities of the reconstruction of basin evolution in the prediction of hydrocarbon prospects), *PhD thesis*, Hungarian Academy of Sciences, Budapest,

Szalay, A., 1988. Maturation and migration of hydrocarbons, SE Pannonian Basin, *Am. Assoc. Petrol. Geol. Mem.*, **45**, 347–354.

Tari, G., Horváth, F. & Rumpler, J., 1992. Styles of extension in the Pannonian Basin, *Tectonophysics*, **208**, 203–219.

Touretzki, D. S. & Pomerleau, D.A., 1989. What's hidden in the hidden layers?, *Byte*, **14**, 227–233.

Van Balen, R. & Cloetingh, S., 1993. Stress-induced fluid flow in rifted basin, in *Diagenesis and Basin Development*, pp. 87–98, eds Horbury, A.D. & Robinson, A.G., Am. Assoc. Petrol. Geol. Studies in Geology, **36**, Tulsa, USA.

Van Balen, R. & Cloetingh, S., 1994. Tectonic control of the sedimentary record and stress-induced fluid flow: constraints from basin modelling, in *Geofluids: Origin, Migration and Evolution of Fluids in Sedimentary Basins*, pp. 9–26, ed. Parnell, J., Spec. Pub. Geol. Soc. Lond., Geological Publishing House, Bath.

Van Balen, R., Lenkey, L., Cloetingh, S. & Horváth, F., 1995. Two-dimensional modelling of stratigraphy and fluid flow in the Pannonian Basin, *Am. Assoc. Petrol. Geol. Bull.*, submitted.

Wu, X. & Zhou, Y., 1993. Reserve estimation using neural network techniques, *Comp. Geosci.*, **19**, 567–575.